Smith–Purcell free electron laser based on the semi-elliptical resonator*

Meng Xian-Zhu(孟现柱)†, Wang Ming-Hong(王明红), and Ren Zhong-Min(任忠民)

School of Physics Science and Information Engineering, Liaocheng University, Liaocheng 252059, *China*

(Received 26 October 2010; revised manuscript received 29 December 2010)

A novel Smith–Purcell (S–P) free electron laser composed of an electron gun, a semi-elliptical resonator, a metallic reflecting grating and a collector, is presented for the first time. This paper studies the characteristics of this device by theoretical analysis and particle-in-cell simulation method. Results indicate that tunable coherent S–P radiation with a high output peak power at millimeter wavelengths can be generated by adjusting the length of the grating period, or adjusting the voltage of the electron beam. The present scheme has the following advantages: the semi-elliptical resonator can reflect all radiation with the emission angle θ and random azimuthal angles, back onto the electron beam with same-phase and causes the electrons to be modulated, so the output power and efficiency are improved.

Keywords: Smith–Purcell radiation, free electron laser, quasi optical resonator

PACS: 07.57.–c, 41.60.Cr, 52.59.Rz, 42.60.Da **DOI:** 10.1088/1674-1056/20/5/050702

1. Introduction

When a sheet electron beam passes close to the surface of the grating, electromagnetic radiation is emitted in all directions. This phenomenon is known as the Smith–Purcell (S–P) effect. The radiation mechanism was predicted by Frank and observed in the visible spectral range for the first time by Smith and Purcell[1] using a 250–300 keV electron beam. Usually, the incoherent radiation from S–P effect is too weak to use and the detection of the signal is very difficult. To generate coherent radiation, a feedback configuration such as open cavity or close cavity is utilized and such experiments have been demonstrated successfully at millimeter and far-infrared wavebands.[2,3] These experiments are important in extending the spectrum and developing tunable coherent radiation. Based on the S–P effect, we have suggested the construction of a laser that generates and amplifies electromagnetic waves. This device is called the S–P free electron laser (FEL),[4−6] which is a promising candidate for developing a more compact, less complex FEL in comparison with conventional magnetic-wiggler FEL.[7,8] In this paper, we present a novel S–P FEL device developed by our group, which is composed of a semi-elliptical resonator, a metallic reflecting grating and a relativistic sheet electron beam with moderate energy. The characteristics of this device are studied by theoretic analysis and particle-in-cell (PIC) simulation method. The present scheme has the following advantages: the semi-elliptical resonator can reflect all radiation with the emission angle θ and random azimuthal angles, back onto the electron beam with same-phase and causes the electrons to be modulated, so the output power and efficiency are improved.

2. Basic theoretical background

In the S–P effect, the wavelength λ of the S–P radiation depends on the S–P radiation formula

$$\lambda = \frac{l}{n}\left(\frac{1}{\beta} - \cos\theta\right), \tag{1}$$

where $\beta = v/c$ is the ratio of the electron's velocity to the velocity of light, l is the length of the grating period, the integer n is the order of the space harmonic wave, θ is the emission angle of observation relative to the electron beam direction. Definition of axes and angles is shown in Fig. 1.[3,9] According to Eq. (1), an S–P radiation at millimeter wavelengths can be generated by adjusting the length of the grating period, adjusting the voltage of the electron beam to moderate energy and adjusting the emission angles. For example, when the length of the grating period $l = 1.5$ mm and energy of electron beam $T = 100$ keV, the wavelength region between 1.236 mm and 4.230 mm can be

*Project supported by the National Natural Science Foundation of China (Grant No. 60871047) and the Natural Science Foundation of Liaocheng University of China (Grant No. X0810018).

†Corresponding author. E-mail: mengxz12@yahoo.com.cn

© 2011 Chinese Physical Society and IOP Publishing Ltd

generated. The effect of spectrum of the S–P radiation on the emission angles is shown in Fig. 2.

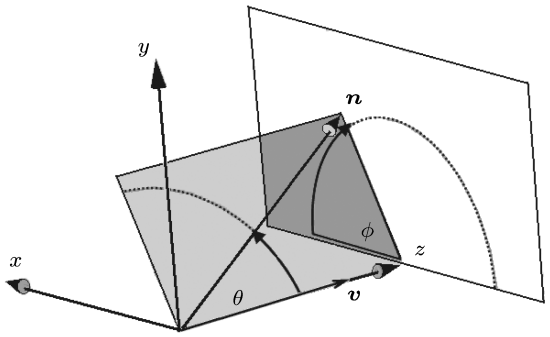


Fig. 1. Definition of axes and angles: the electron beam is propagating in the z direction and the vertical to the grating is along x. The emission and azimuthal angles are θ and ϕ, respectively.

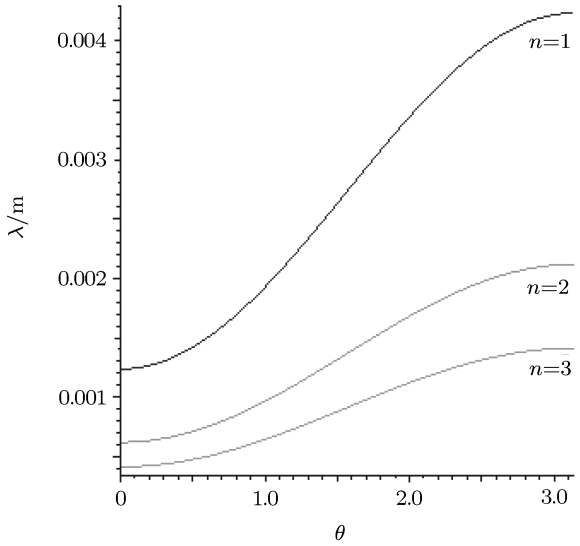


Fig. 2. The effect of spectrum of the S–P radiation on the emission angles.

The angular distribution of the number of photons $\mathrm{d}N$ per electron radiated into the nth order into the solid angle $\mathrm{d}\Omega$ is

$$\frac{\mathrm{d}N}{\mathrm{d}\Omega} = \alpha n N_{\mathrm{W}} \frac{\sin^2\theta\sin^2\phi}{(1/\beta-\cos\theta)^2} \times \exp\left[-\frac{d}{h_{\mathrm{int}}}\zeta(\theta,\phi)\right] R^2, \quad (2)$$

$$\zeta(\theta,\phi) = \sqrt{1+\beta^2\gamma^2\sin^2\theta\sin^2\phi}, \quad (3)$$

where α is the fine-structure constant, N_{W} the number of the grating periods, d is the distance between electron and grating surface. The interaction length is

$$h_{\mathrm{int}} = \frac{\beta\gamma}{4\pi}\lambda, \quad (4)$$

where $\gamma = (1-\beta^2)^{-1/2}$ is the Lorentz factor, describes the characteristic finite range of the virtual photons emitted and reabsorbed by the electrons and the wavelength of the S–P radiation. The term R^2 is a complicated expression that depends on the details of the grating profile and on the wavelength of the radiation. Although an analytic form can be written down for the case of a profile consisting of two straight facets only, it is best to evaluate R^2 numerically.[9]

According to Eq. (2), as a sheet electron beam passes close to the surface of the grating, electromagnetic radiation is emitted in all directions. The intensity decreases exponentially with increasing distance between the electron and grating surface. When the distance between electron and grating surface $d = 0.25$ mm and the transverse size of sheet electron beam $D = 0.3$ mm, the maximum distance between electron and grating surface $d_{\max} = 0.4$ mm, and the minimum distances between electron and grating surface $d_{\min} = 0.1$ mm. The effect of intensity $\mathrm{d}N/\mathrm{d}\Omega$ of the S–P radiation on the emission angles and the azimuthal angles with different distances are shown in Fig. 3. The operating parameters are: the length of the grating period $l = 1.5$ mm, the kinetic energy of electron beam $T = 100$ keV, the distance between electron and grating surface $d = 0.25$ mm and the transverse size of sheet electron beam $D = 0.3$ mm. According to Fig. 3, when the distance between electron and grating surface $d = d_{\max}$, the intensity $\mathrm{d}N/\mathrm{d}\Omega$ of the S–P radiation becomes maximum for the emission angle $\theta \approx 1.85$ and the azimuthal angle $\phi = \pi/2$. According to Eq. (1), the theoretical wavelength of the S–P radiation is $\lambda \approx 3.07$ mm at the emission angle $\theta \approx 1.85$ and the corresponding frequency $\nu \approx 95$ GHz; when the distance between electron and grating surface $d = 0.25$ mm, the intensity $\mathrm{d}N/\mathrm{d}\Omega$ of the S–P radiation becomes maximum for the emission angle $\theta \approx \pi/2$ and the azimuthal angle $\phi = \pi/2$. According to Eq. (1), the theoretical wavelength of the S–P radiation $\lambda \approx 2.736$ mm at the emission angle $\theta \approx \pi/2$ and the corresponding frequency $\nu \approx 109$ GHz; when the distance between the electron and grating surface $d = d_{\min}$, the intensity $\mathrm{d}N/\mathrm{d}\Omega$ of the S–P radiation becomes maximum for the emission angle $\theta \approx 1.3$ and the azimuthal angle $\phi = \pi/2$. According to Eq. (1), the theoretical wavelength of the S–P radiation is $\lambda \approx 2.33$ mm at the emission angle $\theta \approx 1.3$ and the corresponding frequency $\nu \approx 128$ GHz. According to the intensity $\mathrm{d}N/\mathrm{d}\Omega$ in Fig. 3, we also can find that the frequency ($\nu \approx 128$ GHz) is of the dominant radiation.

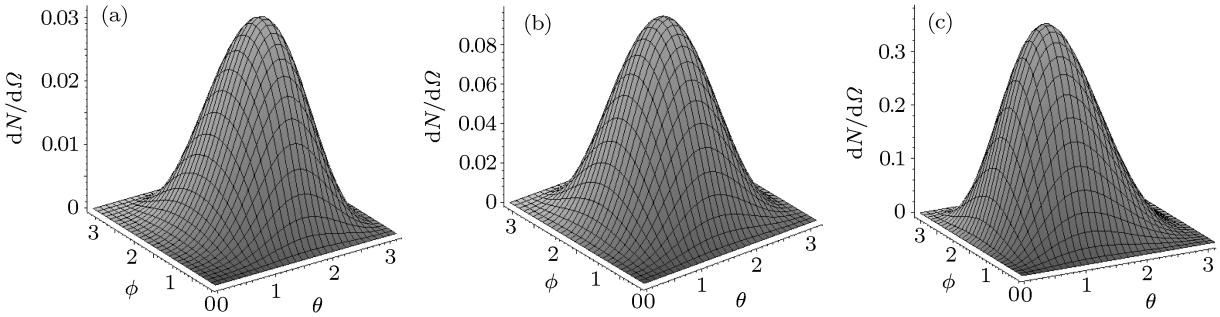


Fig. 3. The effect of intensity $\mathrm{d}N/\mathrm{d}\Omega$ of the S–P radiation on the emission angles and the azimuthal angles. (a) $d_{\max}/l = 0.4/1.5$; (b) $d/l = 0.25/1.5$; (c) $d_{\min}/l = 0.1/1.5$.

3. The theoretical analysis of the quasi optical resonator composed of a pair of semi-conical mirrors

In the S–P effect, the S–P radiation is too weak to use and detection of the signal is very difficult. To generate coherent radiation, a feedback configuration in the S–P FEL is utilized. The classical experimental set-up of S–P FEL is shown in Fig. 4.[10] As a sheet electron beam passes over the metallic reflecting grating, it emits S–P radiation. The resonator reflects the radiation with the emission angle θ and azimuthal angle $\phi = \pi/2$, back onto the electron beam and causes the electrons to be modulated. In this classical S–P FEL, the resonator cannot reflect the radiation with the emission angle θ and other azimuthal angles, back onto the electron beam.

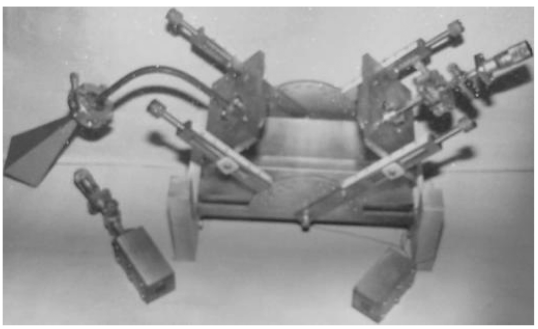


Fig. 4. The classical experimental set-up of S–P FEL.

To reflect all radiation with the emission angle θ and random azimuthal angles, back onto the electron beam, we present a developed novel S–P FEL device. In the novel technical scheme, the S–P FEL is composed of an electron gun, a semi-elliptical resonator, a metallic reflecting grating and a collector. The configuration of FEL is schematically shown in Fig. 5. The semi-elliptical resonator is composed of a semi-elliptical mirror and a metallic reflecting grating. In this S–P FEL, as a sheet electron beam passes over the metallic reflecting grating and along the focal line of elliptical mirror, the electromagnetic radiation is emitted in all directions. The semi-elliptical resonator can reflect all radiation with the emission angle θ and random azimuthal angles, back onto the electron beam with same-phase and causes the electrons to be modulated, so the output power and efficiency are improved.

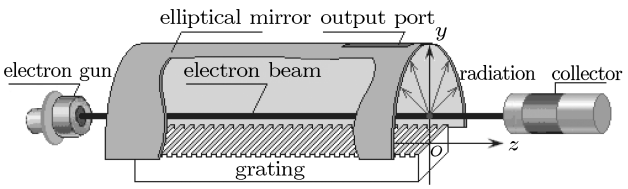


Fig. 5. Schematic diagram of the novel S–P FEL.

The vertical plane of semi-elliptical resonator is shown in Fig. 6.[11] According to the reflective characteristics of elliptical mirror, any ray emitted by the electron beam at the focus, F_1, to the surface of elliptical mirror will be reflected back onto the other focus, F_1', from the surface of elliptical mirror. As shown in Fig. 6, the radiation ray in $x - y$ plane (the emission angle θ equal $\pi/2$), e.g. F_1A, emitted by the electron beam at the focus, F_1, will be reflected back onto the focus, F_1', from the surface of elliptical mirror, e.g. AB. The surface of the grating can be regarded as a flat mirror. According to the law of reflection, the radiation ray, e.g. AB, will be reflected back onto the electron beam from the surface of the grating e.g. BF_1C. And for the same reason, the reflected radiation ray, e.g. BF_1C, will be reflected back onto the focus, F_1', from the surface of elliptical mirror, e.g. CD, etc. The reflected radiation ray, e.g. EG, will be reflected back onto the electron beam from the surface of the grating and toward the output port. The

results show that all radiation rays with the emission angle $\theta = \pi/2$ and random azimuthal angles, emitted by the electron beam at the focus, F_1, can be reflected back onto the electron beam and toward the output port after multiple reflections.

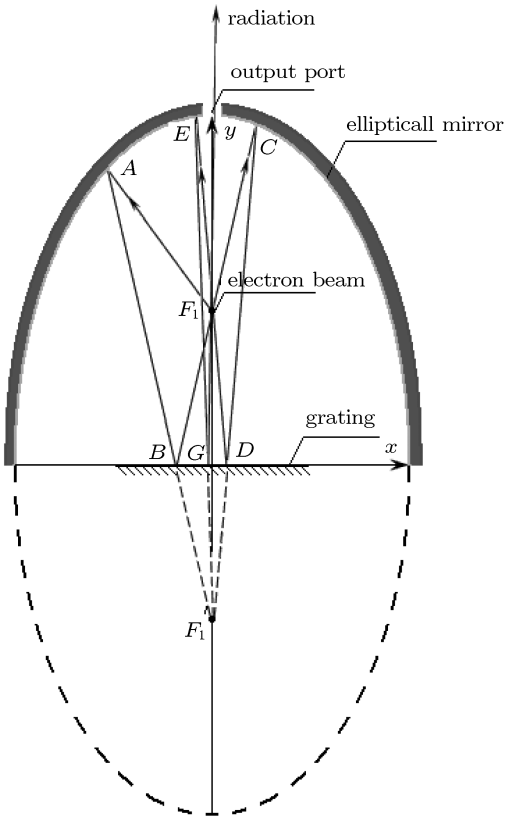


Fig. 6. Vertical plane of semi-elliptical resonator.

As shown in Fig. 6, the equations of the elliptical mirror can be expressed as: $y^2/a^2 + x^2/b^2 = 1$, where a is major half axis and b is minor half axis. In the semi-elliptical resonator, when the radiation ray is reflected back onto the electron beam, the optical path difference of any radiation ray in a cycle, e.g. $F_1A \to AB \to BF_1$, can be expressed as

$$\delta = \sqrt{(y_A - f)^2 + x_A^2} + \sqrt{(y_A - y_B)^2 + (x_A - x_B)^2} + \sqrt{f^2 + x_B^2} = 2a, \quad (5)$$

where f is focal length. The results show that all radiation rays with the emission angle $\theta = \pi/2$ and random azimuthal angles, emitted by the electron beam at the focus, F_1, can be reflected back onto the electron beam with same-phase. When

$$2a = k\lambda, \quad (6)$$

where k is a positive integer, all radiation rays is enhanced by the phase matching so as to produce the high peak power photon target.

It can be proved that if the emission angle $\theta \neq \pi/2$ e.g. $\theta = 1.3$, all radiation rays with the emission angle θ and random azimuthal angles, emitted by the electron beam, still can be reflected back onto the electron beam from the surface of elliptical mirror with same-phase. In this condition, Eq. (6) should be expressed as

$$2a/\sin\theta = k\lambda. \quad (7)$$

When the radiation ray is reflected back onto the electron beam, the electron beam can be modulated. In the semi-elliptical resonator, all radiation with the emission angle θ and random azimuthal angles, can be reflected back onto the electron beam with same-phase and causes the electrons to be modulated better. If the proper conditions of synchronism are met, the electron beam is bunched and the radiation is gained gradually.[10] When the interaction reaches a self-exciting condition, a steady state oscillation is established at one of the resonant frequencies of the semi-elliptical resonator. By adjusting the length of the grating period, or adjusting the voltage of the electron beam, tunable coherent S–P radiation at millimeter wavelengths can be observed.

4. PIC simulation of beam–wave interaction

By the PIC simulation method, we can study the characteristics of the S–P FEL device. The PIC simulations are performed with the CHIPIC code, which is a finite-difference time-domain code for simulating processes involving interactions between space charge and electromagnetic fields.[12–14] With the help of the two-dimensional (2D) PIC simulation, we can observe the characteristics of S–P radiation including the radiation energy and field distribution as well as the interaction processes of electron bunches with the target.[15] According to Eq. (5), all radiation rays in $x-y$ plane of the semi-elliptical resonator, emitted by the electron beam at the focus, F_1, can be reflected back onto the electron beam with same-phase and toward the output port in $z-y$ plane after multiple reflections. So we can study the characteristics in $z-y$ plane of the semi-elliptical resonator by the PIC simulation method instead of the characteristics in all plane of the semi-elliptical resonator. Our group preliminary studied the characteristics in $z-y$ plane of the S–P FEL device by the PIC simulation method. The simulation geometry is shown in Fig. 7. The operating parameters are: electron beam voltage 100 kV; pulse beam current 50 A; the transverse size of sheet electron beam 0.3 mm; the grating with period 1.5 mm,

groove of depth 0.684 mm, width 0.5 mm; the axial magnetic field 2.0 T; the major half axis of the semi-elliptical resonator 16.416 mm.

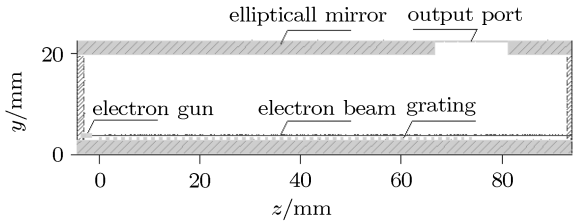


Fig. 7. The simulation geometry.

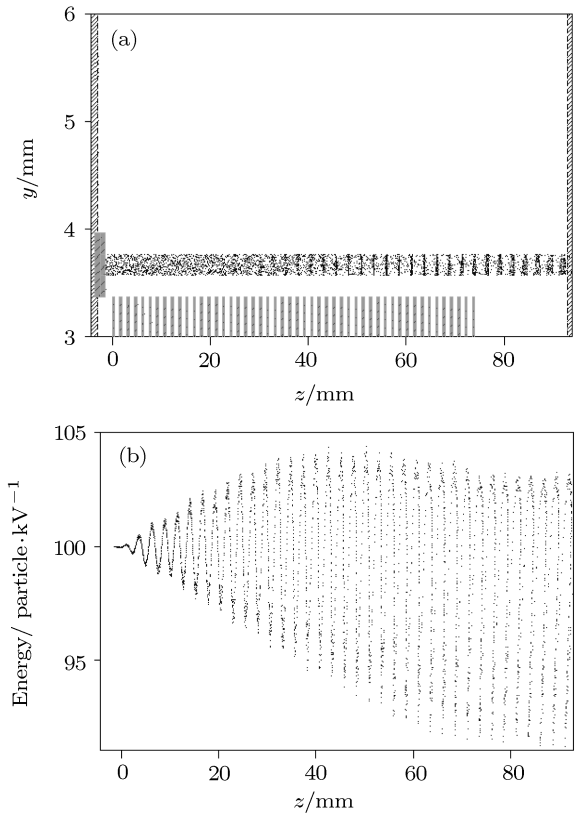


Fig. 8. Phase-space distribution: (a) density of electrons in the $z-y$ plane at 45.664 ns, bunching is evident; (b) kinetic energy of electrons in bunching state.

Figure 8(a) shows the density of electrons in a longitudinal direction when bunching has occurred at time 45.664 ns and Fig. 8(b) shows the kinetic energy of electrons in bunching state at the same time. In Fig. 8, we show a snapshot of the beam just above the grating, along with its distribution in $T-z$ phase space, where T denotes the kinetic energy. Strong bunching is apparent in both. Evidently, a majority of electrons are in the state of losing energy and the high-frequency field is increased in power, correspondingly. By counting oscillations we estimate approximately 2.37 mm for the wavelength, which is quite consistent with the value expected from the dispersion relation. We also note that the mean energy loss is 2–3 keV or 2% to 3% of the beam energy. In Fig. 8(b), we can also find that the well-known two-stream instability[8] is produced owing to the velocity of electrons modulated by radiation electromagnetic wave. Figure 9 gives the profile distribution of field energy in $z-y$ plane of the semi-elliptical resonator. In Fig. 9, a contour map of the electromagnetic field components E_x, E_y, E_z, B_x, B_y and B_z in the $z-y$ plane at time $t = 45.664$ ns is displayed. We can see that the distribution of field displays regular distribution. This kind of filed distribution is beneficial to improving beam–wave interaction. The line integral curve of the electric field (E.DL) and the corresponding fast Fourier transform (FFT) at output port is given by Fig. 10. The line integral curve of the magnetic field (H.DL) and the corresponding FFT at output port is given by Fig. 11. Apparently, there exist two different types of radiation. One is diffraction emission originated from the evanescent wave and diffracted at the ends of grating, whose frequency is the evanescent frequency. The other is the so-called S–P-FEI radiation originated from ordinary S–P radiation but enhanced by the micro-bunching of electron beam in some special direction corresponding to the second harmonic of the evanescent wave.[16] The evolution curve of field power the poynting vector over an area S.DA and the corresponding FFT at output port are shown in Fig. 12. As the beam–wave interaction reaches self-exciting condition, the radiation field begins to increase rapidly. In Fig. 12, the time signal shows rapid growth about after 12 ns. From the FFT amplitude, the dominant radiation is the second harmonic (126.481 GHz), which peaks at the emission angle of about $\theta \approx 1.32$ corresponding to the S–P radiation angle predicted by Eq. (1). Of course, due to the beam–wave interaction which reduces the value of the particle velocity, there is a slight discrepancy between the simulation data for the radiation angle of $\theta \approx 1.32$ and the theoretical value $\theta \approx 1.3$ of the basic S–P equation. If we consider the mean energy loss (3 keV), according to Eq. (1), the practical wavelength of the S–P radiation is $\lambda \approx 2.37$ mm at the emission angle $\theta \approx 1.3$ and the corresponding frequency is $\nu \approx 126.5$ GHz, which is quite consistent with the frequency of the dominant radiation. From the contour plot of Fig. 9, one can easily understand that the dominant second harmonic radiates at the emission angle of about $\theta \approx 1.3$.

It can be concluded from the simulation results that the semi-elliptical resonator can be designed to operate as S–P-FEL. We can also find that millimeter coherent radiation can be generated by employing moderate relativistic electron beam in the semi-elliptical resonator.

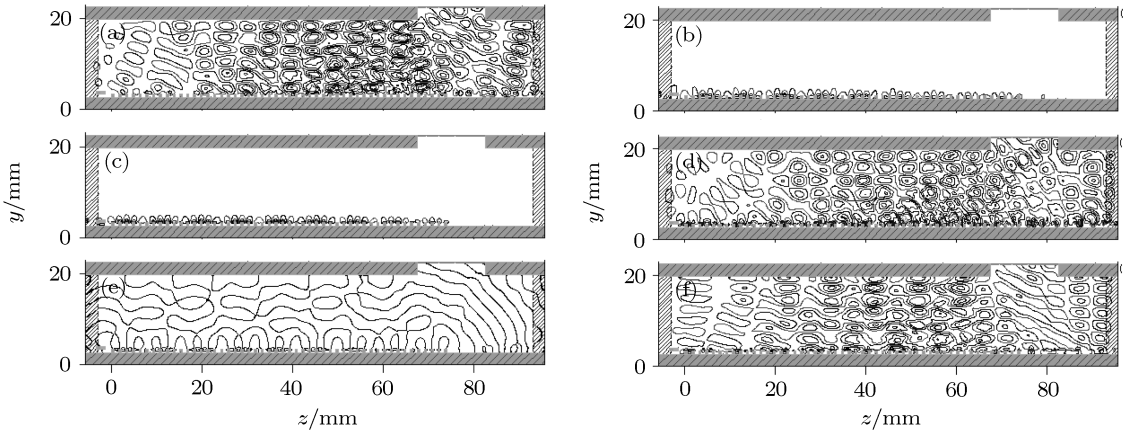


Fig. 9. Profile distribution of field energy. (a) $E_x/\mathrm{V{\cdot}m^{-1}}$, (b) $B_x/10^{-3}$ T, (c) $E_y/10^4$ $\mathrm{V{\cdot}m^{-1}}$, (d) $B_y/10^{-8}$ T, (e) $E_z/10^4$ $\mathrm{V{\cdot}m^{-1}}$, (f) $B_z/10^{-8}$ T.

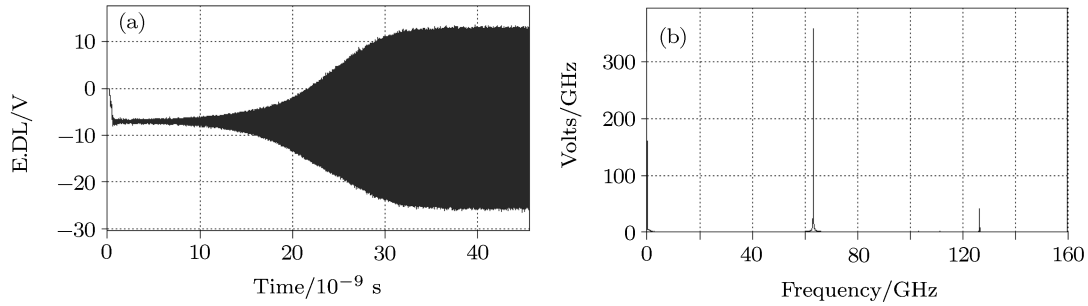


Fig. 10. The operating frequency at output port: (a) the field integral E.DL; (b) the corresponding FFT.

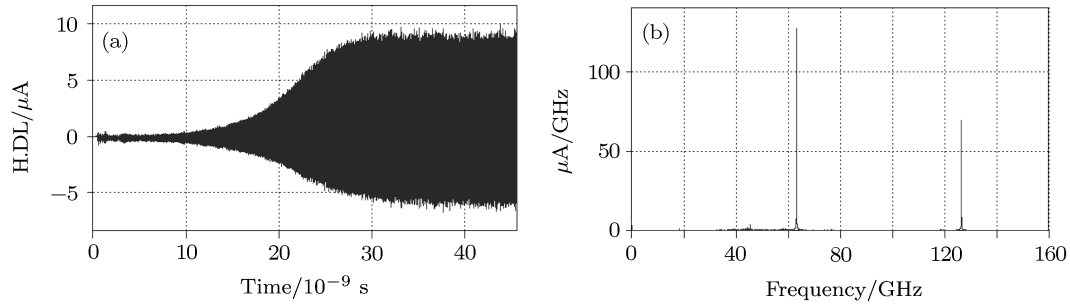


Fig. 11. The operating frequency at output port: (a) the field integral H.DL; (b) the corresponding FFT.

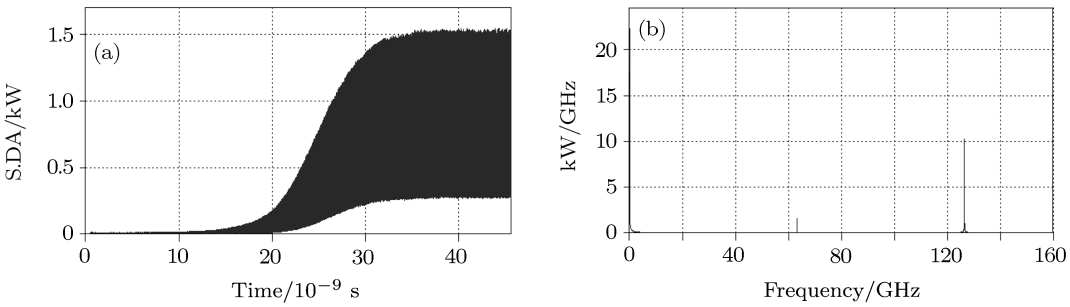


Fig. 12. The evolution curve of field power at output port: (a) the field power S.DA; (b) the corresponding FFT.

5. Conclusions

An S–P FEL composed of an electron gun, a semi-elliptical resonator, a metallic reflecting grating and a collector, is presented for the first time. The characteristics of this device are studied by theoretical analysis and PIC simulation method. Results indicate that tunable coherent S–P radiation with a high output peak power at millimeter wavelengths can be generated by adjusting the length of the grating period, or adjusting the voltage of the electron beam. The present scheme has the following advantages: the semi-elliptical resonator can reflect all radiation with the emission angle θ and random azimuthal angles, back onto the electron beam with same-phase and causes the electrons to be modulated, so the output power and efficiency are improved.

References

[1] Smith S J and Purcell E M 1953 *Phys. Rev.* **92** 1069

[2] Chen J Y, Liang Z, Zhang Y C and Yang Z Q 2001 *Int. J. Electron.* **88** 467

[3] Doriaa A, Galleranoa G P, Giovenalea E, Messinaa G, Doucasb G, Kimmittc M F andrewsd H L and Brownell J H 2002 *Nucl. Instrum. Methods* A **483** 263

[4] Urata J, Goldstien M and Kimmitt M F 1998 *Phys. Rev. Lett.* **80** 515

[5] Liu C S and Tripathi V K 1998 *IEEE J. Quantum Electron.* **34** 1503

[6] Wachtel J M 1979 *J. Appl. Phys.* **50** 49

[7] Andrews H L, Boulware C H, Brau C A and Jarvis J D 2005 *Phys. Rev. ST Accel. Beams* **8** 110702

[8] Marshall T C 1985 *Free Electron Lasers* (New York: Macmillan Publishing Company)

[9] Backe H, Lauth W, Mannweiler H, Rochholz H, Aulenbacher K, Barday R, Euteneuer H, Kaiser K H, Kube G, Schwellnus F and Tioukine V 2006 *Advanced Radiation Sources and Applications* (NATO Science Series II: Mathematics, Physics and Chemistry) **199** 267

[10] Wang M H, Liu P K, Ge G Y and Dong R X 2007 *Optics & Laser Technology* **39** 1254

[11] Meng X Z, Wang M H and Ren Z M 2010 *Acta Phys. Sin.* **59** 1638 (in Chinese)

[12] Gao X, Yang Z Q, Qi L M, Lan F, Shi Z J, Li D Z and Liang Z 2009 *Chin. Phys.* B **18** 2452

[13] Zhang K C, Wu Z H and Liu S G 2008 *Chin. Phys.* B **17** 3402

[14] Lai G J and Liu P K 2007 *Acta Phys. Sin.* **56** 4515 (in Chinese)

[15] Liu W X, Tang C X and Huang W H 2010 *Chin. Phys.* B **19** 062902

[16] Bei H, Dai D D and Dai Z M 2008 *High Power Laser & Particle Beams* **20** 2067